

Early Optical Afterglows from Wind-Type Gamma-Ray Bursts

Shiho Kobayashi^{1,2} and Bing Zhang¹

¹*Department of Astronomy & Astrophysics, Pennsylvania State University, University Park, PA 16802*

²*Center for Gravitational Wave Physics, Pennsylvania State University, University Park, PA 16802*

ABSTRACT

We study prompt optical emission from reverse shocks in the wind-type gamma-ray bursts. The emission is evaluated in both the thick and thin shell regimes. We discuss the angular time delay effect and the post-shock evolution of the fireball ejecta, which determine the decay index of the prompt optical emission and the duration of the radio flare. We discuss distinct emission signatures of the wind environment compared with the constant interstellar medium environment. We also present two recipes for directly constraining the initial or early time Lorentz factor of the fireball using the reverse and forward shock optical afterglow data for the wind case.

Subject headings: gamma rays: bursts - hydrodynamics - relativity - shock waves

1. Introduction

The gamma-ray burst (GRB) afterglow observations are usually explained by a model in which a relativistic fireball shell (ejecta) is expanding into a uniform interstellar medium (ISM). However, there is observational evidence suggesting a link between GRBs and massive stars or star formation (e.g. Mészáros 2001 for a review). An important consequence of a massive star origin for the afterglow is that the fireball shell should be expanding into a pre-burst stellar wind of the progenitor star with a density distribution of $\rho \propto R^{-2}$ (e.g. Chevalier & Li 1999; Mészáros, Rees & Wijers 1998; Dai & Lu 1998). This wind model is discussed to be consistent with some GRB afterglow data (Chevalier & Li 1999, 2000).

It is expected that many early optical afterglows will be discovered soon in the observational campaigns led by HETE-2 and Swift. Long time span (from right after the GRB trigger to a year) observation data will allow us to distinguish differences between the ISM and wind models clearly.

In this Letter, we will discuss the optical reverse shock emission for the wind model in detail. The previous study (Chevalier & Li 2000) gave the discussions for the thick shell case, and we will consider both the thin and thick shell cases. We show that the angular time delay effect plays an important role in discussing the lightcurve decaying phase of the reverse shock emission.

2. The Model

We consider a relativistic shell (fireball ejecta) with an isotropic energy E , an initial Lorentz factor η and an initial width Δ_0 expanding into a surrounding medium with density distribution of $\rho = AR^{-2}$. If the GRB progenitor is a massive star, the strong stellar wind could produce such an inhomogeneous density distribution (wind model). In this paper, Lorentz factors γ , radii R and widths Δ are measured in the laboratory frame where the progenitor is at rest. The observer is also in this frame if the cosmological expansion is neglected. Thermodynamic quantities: mass densities ρ and internal energy e are measured in the fluid comoving frame.

The interaction between the shell and the wind is described by two shocks: a forward shock propagating into the wind and a reverse shock propagating into the shell. The shocks accelerate electrons in the shell and wind material, and the electrons emit photons via synchrotron process. The spectrum of each shock emission is described by a broken power law with a peak $F_{\nu, \max} \propto N_e B \gamma$ and break frequencies: a typical frequency $\nu_m \propto B \gamma \gamma_m^2$ and a cooling frequency $\nu_c \propto 1/B^3 \gamma t^2$ (Sari, Piran & Narayan 1998) where N_e is the number of electrons accelerated by the shock, B is the magnetic field strength behind the shock, γ and γ_m are the bulk Lorentz factor of the shocked material and the random Lorentz factor of the typical electrons in the shocked material, respectively. Assuming that constant fractions (ϵ_e and ϵ_B) of the internal energy e produced by the shock go into the electrons and the magnetic field, we get

$$\nu_m \propto \gamma \rho^{-2} e^{5/2}, \quad \nu_c \propto \gamma^{-1} e^{-3/2} t^{-2}, \quad F_{\nu, \max} \propto N_e \gamma e^{1/2}. \quad (1)$$

The light curve at a fixed frequency (e.g. optical band) depends on the temporal evolution of the break frequencies and the peak power. When the hydrodynamics of the shocked material is determined, eq. (1) gives the temporal evolution.

3. Forward Shock

Observations of optical afterglows usually start around several hours after the burst trigger. At such a late time, the shocked wind material forms a relativistic blast wave and carries almost all the energy of the system. Chevalier & Li (1999) gave the characteristics of the forward shock (blast wave) emission as follows,

$$\nu_{m,f}(t) \sim 1.6 \times 10^{12} \zeta^{1/2} \epsilon_{e,-1}^2 \epsilon_{B,-2}^{1/2} E_{52}^{1/2} t_d^{-3/2} \text{ Hz}, \quad (2)$$

$$\nu_{c,f}(t) \sim 6.3 \times 10^{13} \zeta^{-3/2} \epsilon_{B,-2}^{-3/2} E_{52}^{1/2} A_*^{-2} t_d^{1/2} \text{ Hz}, \quad (3)$$

$$F_{\nu,max,f}(t) \sim 6.3 d^{-2} \zeta^{1/2} \epsilon_{B,-2}^{1/2} E_{52}^{1/2} A_* t_d^{-1/2} \text{ mJy}, \quad (4)$$

where $\zeta = (1+z)/2$, $d = (\sqrt{1+z}-1)/(\sqrt{2}-1)$, z is the redshift of the burst, $\epsilon_{e,-1} = \epsilon_e/0.1$, $\epsilon_{B,-2} = \epsilon_B/0.01$, $E_{52} = E/10^{52}$ ergs, $A_* = A/5 \times 10^{11} \text{ g cm}^{-1}$, t_d is the observer's time in units of days. The optical flux from the forward shock decays proportional to $t^{-1/4}$ initially, and decays faster as $t^{-(3p-2)/4}$ after a transition of $\nu_{m,f}$ through the optical band $\nu_R \sim 5 \times 10^{14} \text{ Hz}$ (Chevalier & Li 2000) where p is the index of the power law distribution of the accelerated electrons. Using $\nu_{R*} = \nu_R/5 \times 10^{14} \text{ Hz}$, the break time $t_{m,f}$ (the passage of $\nu_{m,f}$) and the optical flux (in the fast-cooling regime) at that time are

$$t_{m,f} \sim 30 \zeta^{1/3} \epsilon_{e,-1}^{4/3} \epsilon_{B,-2}^{1/3} E_{52}^{1/3} \nu_{R*}^{-2/3} \text{ min}, \quad (5)$$

$$F_{\nu_{R,f}}(t_{m,f}) \sim 6 d^{-2} \zeta^{-1/3} \epsilon_{e,-1}^{-1/3} \epsilon_{B,-2}^{-1/3} E_{52}^{2/3} \nu_{R*}^{-1/3} \text{ mJy}, \quad (6)$$

4. Reverse Shock

At earlier time when the reverse shock crosses the shell, the forward-shocked wind and the reverse shocked shell carry comparable amount of energy. A significant emission is expected from the reverse shock also (Mészáros & Rees 1997; Sari & Piran 1999a). During the reverse shock crosses the shell, there are four regions separated by the two shocks: the wind (denoted by the subscript 1), the shocked wind (2), the shocked shell material (3) and the unshocked shell material (4). Using the jump conditions for the shocks and the equality of pressure and velocity along the contact discontinuity, we can estimate the Lorentz factor γ_i , the internal energy e_i and the mass density ρ_i in the shocked regions as functions of three variables $\gamma_4 (= \eta)$, ρ_1 and ρ_4 (e.g. Blandford & McKee 1976).

There are two limits to get a simple analytic solution to the hydrodynamic quantities at a shell radius R (Sari and Piran 1995). If the Lorentz factor is low $\eta^2 \ll f$ where $f = \rho_4/\rho_1$, the reverse shock is Newtonian which means that the Lorentz factor of the shocked shell material is almost unity in the frame of the unshocked shell material. It is too weak to slow

down the shell effectively so that $\gamma_3 \sim \eta$. On the other hand, if the Lorentz factor is high $\eta^2 \gg f$, the reverse shock is relativistic, and considerably decelerates the shell material, hence $\gamma_3 \sim \eta^{1/2} f^{1/4}$.

4.1. Critical Radii

Since the density ratio f is generally a function of R , there is a possibility that the reverse shock evolves from Newtonian to relativistic during the propagation. The evolution of the reverse shock depends on the ratio of two radii: $R_\gamma \equiv E/4\pi A c^2 \eta^2$ where the forward shock sweeps a mass of $E/c^2 \eta^2$ and $R_s \equiv \Delta_0 \eta^2$ where the shell begins to spread if the initial Lorentz factor varies by order η (Sari & Piran 1995; Kobayashi, Piran & Sari 1999). Another important radius is R_x where the reverse shock crosses the shell. The lab-frame time it takes for the reverse shock to cross a width dx of the shell material is given by (Sari & Piran 1995),

$$dt_{lab} \sim \frac{dR}{c} \sim \eta f^{1/2} \frac{dx}{c}. \quad (7)$$

We can regard R/c as time t_{lab} in the laboratory frame because of the highly relativistic expansion of the shell. Since the whole shell width is $\Delta \sim \max[\Delta_0, R/\eta^2]$, we obtain $R_x \sim \max[(R_s R_\gamma)^{1/2}, R_\gamma]$.

Considering the following relation between η^2/f and the radii, we can classify the evolution of reverse shocks into two cases by using a critical Lorentz factor $\eta_c \equiv (E/4\pi A c^2 \Delta_0)^{1/4}$ (see Sari & Piran 1995 and Kobayashi & Zhang 2003 for the ISM model).

$$\frac{\eta^2}{f} = \max\left[\frac{R_s}{R_\gamma}, \frac{R}{R_\gamma}\right]. \quad (8)$$

If $R_s/R_\gamma = (\eta/\eta_c)^4 > 1$ (Thick Shell Case), the reverse shock is relativistic from the beginning (at the end of the GRB phase), which is different from the ISM model in which the reverse shock only becomes relativistic later. The reverse shock crosses the shell at $R_x \sim (R_s R_\gamma)^{1/2}$ before the shell begins to spread at R_s . The reverse shock significantly decelerates the shell material $\gamma_3 \sim \eta_c$. If $R_s/R_\gamma < 1$ (Thin Shell Case), the reverse shock is initially Newtonian and becomes only mildly relativistic when it traverses the shell at $R_x \sim R_\gamma$. We can regard γ_3 as constant ($\sim \eta$) during the shock crossing.

4.2. Synchrotron Emission

When we observe the emission from the expanding shell, the observer time $t \equiv (1+z)R/c\gamma^2$ is proportional to R , because the Lorentz factor of the shocked shell during the

shock crossing $\gamma_{\times} \sim \min[\eta, \eta_c]$ is constant. By using the shock jump conditions and eq. (7), one finds the scalings before the crossing time $t_{\times} = (1+z)R_{\times}/c\gamma_{\times}^2$,

$$e_3 \propto t^{-2}, \quad \rho_3 \propto t^{-2}, \quad N_e \propto t \quad (\text{thick shell}) \quad (9)$$

$$e_3 \propto t^{-2}, \quad \rho_3 \propto t^{-3}, \quad N_e \propto t^{1/2} \quad (\text{thin shell}). \quad (10)$$

Substituting these scalings to eq. (1), we obtain

$$\nu_{m,r} \propto t^{-1}, \quad \nu_{c,r} \propto t, \quad F_{\nu,max,r} \propto t^0 \quad (\text{thick shell : } t < t_{\times}), \quad (11)$$

$$\nu_{m,r} \propto t, \quad \nu_{c,r} \propto t, \quad F_{\nu,max,r} \propto t^{-1/2} \quad (\text{thin shell : } t < t_{\times}). \quad (12)$$

The initial shell width Δ_0 is given by the intrinsic duration of the GRB, $\Delta_0 \sim (1+z)^{-1}cT$ (Kobayashi, Piran & Sari 1997), the shock crossing time t_{\times} and the critical Lorentz factor can be written in the following forms,

$$t_{\times} \sim \left(\frac{\gamma_{\times}}{\eta_c} \right)^{-4} T, \quad (13)$$

$$\eta_c \sim 60 \zeta^{1/4} E_{52}^{1/4} A_*^{-1/4} T_1^{-1/4}, \quad (14)$$

where $T_1 = T/10\text{sec}$. We can determine the critical Lorentz factor η_c from the observations of the GRB and afterglow. If we detect the shock crossing time t_{\times} (the reverse shock peak time), the Lorentz factor during the shock crossing time γ_{\times} can be estimated from eq. (13).

The spectral characteristics of the reverse shock emission at t_{\times} are related to those of the forward shock emission by the following simple formulae (Kobayashi & Zhang 2003),

$$\nu_{m,r}(t_{\times}) \sim \frac{\eta^2}{\gamma_{\times}^4} \nu_{m,f}(t_{\times}), \quad \nu_{c,r}(t_{\times}) \sim \nu_{c,f}(t_{\times}), \quad F_{\nu,max,r}(t_{\times}) \sim \frac{\gamma_{\times}^2}{\eta} F_{\nu,max,f}(t_{\times}). \quad (15)$$

Using eqs. (2), (3) and (4), we get

$$\nu_{m,r}(t_{\times}) \sim \begin{cases} 4.0 \times 10^{15} \zeta^{-1/2} \epsilon_{e,-1}^2 \epsilon_{B,-2}^{1/2} E_{52}^{-1/2} A_* T_1^{-1/2} \left(\frac{\eta}{200} \right)^2 \text{ Hz} & (\text{thick shell}) \\ 3.6 \times 10^{14} \zeta^{-1} \epsilon_{e,-1}^2 \epsilon_{B,-2}^{1/2} E_{52}^{-1} A_*^{3/2} \left(\frac{\eta}{60} \right)^4 \text{ Hz} & (\text{thin shell}) \end{cases} \quad (16)$$

$$\nu_{c,r}(t_{\times}) \sim \begin{cases} 6.8 \times 10^{11} \zeta^{-3/2} \epsilon_{B,-2}^{-3/2} E_{52}^{1/2} A_*^{-2} T_1^{1/2} \text{ Hz} & (\text{thick shell}) \\ 6.8 \times 10^{11} \zeta^{-1} \epsilon_{B,-2}^{-3/2} E_{52} A_*^{-5/2} \left(\frac{\eta}{60} \right)^{-2} \text{ Hz} & (\text{thin shell}) \end{cases} \quad (17)$$

$$F_{\nu,max,r}(t_{\times}) \sim \begin{cases} 11 d^{-2} \zeta \epsilon_{B,-2}^{1/2} E_{52} A_*^{1/2} T_1^{-1} \left(\frac{\eta}{200} \right)^{-1} \text{ Jy} & (\text{thick shell}) \\ 35 d^{-2} \epsilon_{B,-2}^{1/2} A_*^{3/2} \left(\frac{\eta}{60} \right)^3 \text{ Jy} & (\text{thin shell}) \end{cases} \quad (18)$$

For our typical parameters, the reverse shock emission is in the fast cooling regime $\nu_{c,r} < \nu_{m,r}$ during the shock crossing. So for $t < t_{\times}$, the optical flux from the reverse shock increases

as $\propto t^{1/2}$ for thick shell case (Chevalier & Li 2000), and $\propto t^{(p-1)/2}$ for thin shell case. Since the Lorentz factor of the forward-shocked material is also constant during shock crossing, the optical emission from the forward shock evolves as $t^{1/2}$ at $t < t_{\times}$. But this component is usually masked by the reverse shock emission.

At the shock crossing time t_{\times} , the optical flux reaches the peak. Since for our typical parameter, $\nu_{m,r}(t_{\times})$ is above the optical band ν_R in the thick shell case, while $\nu_{m,r}(t_{\times}) < \nu_R$ in the thin shell case, the peak flux is given by

$$F_{\nu_R,r}(t_{\times}) \sim \left\{ \begin{array}{ll} 0.4 d^{-2} \zeta^{1/4} \epsilon_{B,-2}^{-1/4} E_{52}^{5/4} A_*^{-1/2} T_1^{-3/4} \nu_{R*}^{-1/2} \left(\frac{\eta}{200}\right)^{-1} \text{Jy} & (\text{thick shell}) \\ 1.0 d^{-2} \zeta^{-5/4} \epsilon_{e,-1}^{3/2} \epsilon_{B,-2}^{1/8} E_{52}^{-1/4} A_*^{11/8} \nu_{R*}^{-5/4} \left(\frac{\eta}{60}\right)^5 \text{Jy} & (\text{thin shell}) \end{array} \right\}, \quad (19)$$

where $p = 2.5$ was assumed to derive the equation for the thin shell case.

Generally, using the time dependences of $\nu_{m,f}(t)$, $\nu_{c,f}(t)$ and $F_{\nu,max,f}(t)$ as well as eq. (15), we can relate this peak flux with the optical flux of the forward shock at the break time $t_{m,f}$, i.e.,

$$F_{\nu_R,r}(t_{\times}) \sim \left(\frac{\gamma_{\times}^2}{\eta}\right)^{2-a} \left(\frac{t_{\times}}{t_{m,f}}\right)^{(2-3a)/4} F_{\nu_R,f}(t_{m,f}). \quad (20)$$

where $a = p$ if $\nu_{m,r}(t_{\times})$ is below the optical band, and $a = 1$ if it is above. Detection of the peak ($t_{\times}, F_{\nu_R,r}(t_{\times})$) and the break ($t_{m,f}, F_{\nu_R,f}(t_{m,f})$) will give a constraint to the initial Lorentz factor η . A similar recipe has been proposed by Zhang, Kobayashi & Mészáros (2003) for the ISM case.

4.3. Angular Time Delay Effect

The cooling frequency $\nu_{c,r}(t_{\times})$ is well below the optical band for our typical parameters, the optical emission from the reverse shock should “vanish” after the peak. However, the angular time delay effect prevents abrupt disappearance (this effect was considered for prompt gamma-ray emission or forward shock emission by Fenimore, Madras & Nayakshin 1996; Kobayashi et al. 1997; Kumar & Panaitescu 2000b; Ioka & Nakamura 2001; Ryde & Petrosian 2002; Nakar & Piran 2003).

During the shock crossing $t < t_{\times}$, the observer mainly detect photons emitted up to an angle of $\sim 1/\gamma_{\times}$ relative to the line of sight because of the relativistic beaming effect. The emission above the cooling frequency disappears when the shock passes over the shell at R_{\times} . The observer time delay between photons emitted simultaneously at R_{\times} , one on the line of sight and the other from the direction with an angle θ from the line-of-sight is $\delta t \sim (1 - \mu)R_{\times}/c$ where $\mu \equiv \cos \theta$. The observer continues to receive photons even after t_{\times} .

Let us consider an emitting shell expanding with a Lorentz factor $\gamma_{\times} = (1 - \beta_{\times}^2)^{-1/2} \gg 1$. A general formula to calculate the observed flux from an optically thin shell is derived by Granot, Piran and Sari (1998). Let us use a spherical system (r, θ, ϕ) and time t_{lab} in the Laboratory frame where the $\theta = 0$ axis points toward the observer. Suppose the GRB is at a distance l . The flux at the observer is given by

$$F_{\nu}(t) = \frac{1}{2l^2} \int_0^{\infty} dt_{lab} \int_0^{\infty} dr \int_{-1}^1 d\mu r^2 P'_{\nu'}(r, t_{lab}) \mathcal{D}^2 \delta(t_{lab} - t - r\mu/c) \quad (21)$$

where $\mathcal{D} = [\gamma_{\times}(1 - \beta_{\times}\mu)]^{-1}$, $P'_{\nu'}$ is the rest frame spectral power, $\nu' = \nu/\mathcal{D}$, we have ignored the cosmological time dilation effect which is not important to derive the decay index of the reverse shock emission. The shell width is much smaller than the radius. We apply a thin shell approximation to $P'_{\nu'}$. The main contribution to the integration comes from $r \sim R_{\times}$, because $r^2 P'_{\nu'}$ is a rapidly increasing function of r . Assuming $P'_{\nu'} \propto \nu'^b \delta(r - ct_{lab}) \delta(t_{lab} - R_{\times}/c)$, we obtain $F_{\nu} \propto t^{-2+b}$.

In the local frame, the spectral power is described by a broken power law with a low and high frequency indices $-1/2$ and $-p/2$ and the break frequency $\nu'_{m,r}(R_{\times}) \equiv \nu_{m,r}(t_{\times})/\gamma_{\times}$. The blue shifted one $\mathcal{D}(\mu = 1 - ct/R_{\times})\nu'_{m,r}(R_{\times})$ passes through the optical band ν_R at time $t_b \sim t_{\times}\nu_{m,r}(t_{\times})/\nu_R$. The optical flux initially evolves as $t^{-5/2}$ and decays as $t^{-(p+4)/2}$ after the passage.

Since the forward shock emission decays slower $t^{-1/4}$, it begins to dominate the optical band at $t_{trans} \sim (t_{\times}^{4\alpha}/t_{m,f})^{1/(4\alpha-1)} [F_{\nu_{R,r}}(t_{\times})/F_{\nu_{R,f}}(t_{m,f})]^{4/(4\alpha-1)}$ where we assumed that the optical reverse shock emission decays proportional to $t^{-\alpha}$. For our typical parameters, α is $5/2$ in the thick shell case, and $13/4$ ($p=2.5$) in the thin shell case (see fig 1(a) in which $\alpha \sim 3$ is applied).

$$t_{trans} \sim \left\{ \begin{array}{ll} 37 \zeta^{-2/9} E_{52}^{2/9} A_*^{-2/9} T_1^{7/9} \left(\frac{\eta}{200}\right)^{-4/9} \text{ sec} & (\text{thick shell}) \\ 36 \zeta^{3/4} \epsilon_{e,-1}^{1/2} \epsilon_{B,-2}^{-8/3} E_{52}^{3/4} A_*^{-15/24} \nu_{R*}^{-1/4} \left(\frac{\eta}{60}\right)^{-8/3} \text{ sec} & (\text{thin shell}) \end{array} \right\}. \quad (22)$$

For the typical parameters, the optical emission from the reverse shock drops below that from the forward shock within a minute. However, in a long burst (thick shell) or an energetic one (thin shell), it can dominate in the optical band for a longer time.

4.4. Duration

If the fireball ejecta is collimated in a jet with an opening angle θ_j , the duration of the reverse shock emission is $t_{ang} \sim (1+z)\theta_j^2 R_{\times}/c$. The opening angle θ_j might be determined

from the observations of the blast wave (forward shock) emission. As the blast wave decelerates $\gamma \sim \gamma_x(t/t_x)^{-1/4}$, the size of the visible region increases. The entire jet surface becomes visible to the observer at time $t_j \sim (\theta_j \gamma_x)^4 t_x$. The lack of emitting fluid outside the jet opening leads to a faster afterglow decay and it results in a break of the afterglow light curve at t_j (Rhoads 1999; Sari, Piran & Halpern 1999), even though this break in the wind model may not be as clear as that in the ISM model (Kumar & Panaitescu 2000a; Gou et al. 2001).

$$t_{ang} \sim (t_x t_j)^{1/2} \sim 35 \left(\frac{t_x}{50 \text{ sec}} \right)^{1/2} \left(\frac{t_j}{1 \text{ day}} \right)^{1/2} \text{ min} \quad (23)$$

At a low frequency $\nu < \nu_{c,r}(t_x)$, the observer receives photons from the fluid element on the line of the sight until a break frequency ν_{cut} , which is equal to $\nu_{c,r}(t_x)$ at t_x , crosses the observational band. We now consider this time scale. After the reverse shock crosses the shell, the profile of the forward-shocked wind begins to approach the Blandford-McKee (BM) solution (Blandford & McKee 1976; Kobayashi, Piran & Sari 1999). Since the shocked shell is located not too far behind the forward shock, it roughly fits the BM solution. A given fluid element in a blast wave evolves with a bulk Lorentz factor of $\gamma \propto R^{-3/2}$. Since the observer time is given by $t = R/\gamma^2 c$, we obtain $\gamma \propto t^{-3/8}$. Similarly, the mass density and the internal energy evolve as $\rho \propto R^{-9/2} \propto t^{-9/8}$ and $e \propto R^{-6} \propto t^{-3/2}$, respectively. Assuming that the electron energy and the magnetic field energy remains constant fractions of the internal energy density of the shocked shell, the emission frequency of each electron with γ_e drops quickly with time according to $\nu_e \propto B\gamma\gamma_e^2 \propto t^{-15/8}$ because of the shell expansion. Once the reverse shock crosses the shell, no new electrons are accelerated ($N_e = \text{constant}$). The reverse shock spectrum at $t > t_x$ is described by a power law spectrum $F_{\nu,r} = F_{\nu,max,r}(\nu/\nu_{cut})^{1/3}$ ($\nu < \nu_{cut}$) where $\nu_{cut} = \nu_{c,r}(t_x)(t/t_x)^{-15/8}$ and $F_{\nu,max,r} \propto t^{-9/8}$. The light curve at a low frequency $\nu < \nu_{cut}(t_x)$ decays as $t^{-1/2}$ until ν_{cut} passes through the observational frequency ν at

$$t_{cut} \sim 12\zeta^{-4/5} \epsilon_{B,-2}^{-4/5} E_{52}^{4/15} A_*^{-16/15} \left(\frac{\nu}{10 \text{ GHz}} \right)^{-8/15} \left(\frac{t_x}{50 \text{ sec}} \right)^{19/15} \text{ min.} \quad (24)$$

Though at radio band and early times, self-absorption takes an important role and significantly reduces the flux (Sari & Piran 1999a), $t_{dur} = \max[t_{ang}, t_{cut}]$ can give a rough estimate of the duration of the radio reverse shock emission.

5. Case Studies

GRB 990123: The prompt optical flash from GRB 990123 reached to the peak of ~ 1 Jy about $t_x \sim 50$ sec after the burst trigger and decayed as t^{-2} (Akerlof et al. 1999). This

optical flash and the radio flare detected 1 day after the burst (Kulkarni 1999) are explained well by a reverse shock emission in the ISM model (Sari & Piran 1999b; Kobayashi & Sari 2000). The basic parameters of this burst include (e.g. Kobayashi & Sari 2000 and reference therein) $E_{52} \sim 140$, $z \sim 1.6$, $T_1 \sim 6.3$. We now apply the wind model to the burst. Since the peak time t_x is comparable to the GRB duration, the burst should be a thick shell case. The Lorentz factor of the shell at t_x is $\eta_c \sim 140A_*^{-1/4}$. The optical peak flux is estimated as $F_{\nu_{R,r}}(t_x) \sim 8.1 \epsilon_{e,-1}^{3/2} \epsilon_{B,-2}^{1/8} A_*^{1/4} (\eta/200)^{1/2}$ Jy ($p = 2.5$). The wind model can reproduce the bright optical flash. However, it predicts a flatter rising of $t^{1/2}$ or $t^{(p-1)/2}$ compared to $t^{3/4}$ evaluated from the first two ROTSE data, and a steeper decline of $t^{-5/2}$ or $t^{-(p+4)/2}$ after the peak (Chevalier & Li 2000). The optical reverse shock emission is expected to be overtaken by that from the forward shock at $t_{trans} \sim 6.5 \epsilon_{e,-1}^{1/2} \epsilon_{B,-2}^{1/8} A_*^{1/12} (\eta/200)^{1/6}$ min, but the observed flash decays as a single power law of t^{-2} until it falls off below the detection threshold at ~ 11 min. Since the jet break was observed around $t_j \sim 2$ day after the burst (Kulkarni et al 1999), we obtain $t_{ang} \sim 50$ min and $t_{cut} \sim 36 \epsilon_{B,-2}^{-4/5} A_*^{-16/15} (\nu/10\text{GHz})^{-8/15}$ min. In the wind model, the reverse shock emission should disappears well before the radio flare at ~ 1 day.

GRB 021004: The prompt localisation of GRB 021004 by HETE2 allowed the follow up of the afterglow at a very early time and revealed the peculiarity, a major bump around ~ 0.1 days after the burst and a short timescale variability around ~ 1 day. The latter could be interpreted as the result of the forward shock encountering an external medium of variable density or late time energy injections (Lazzati et al. 2002; Nakar, Piran & Granot 2003; Heyl & Perna 2003; Fox et al. 2003). In the frame work of the ISM model, it was shown that the major bump could be explained by the passage of the typical frequency of the forward shock emission through the optical band, and that the early time optical emission is a combination of reverse and forward shock emissions (Kobayashi & Zhang 2003). In the wind model, the optical light curve of the forward shock emission initially behaves as $t^{-1/4}$ and decays steeper as $t^{-(3p-2)/4}$ after the typical frequency crosses the optical band. The bump might be explained by this passage of $\nu_{m,f}$ ¹. The basic parameters of this burst are (e.g. Kobayashi & Zhang 2002 and reference therein) $E_{52} \sim 5.6$, $z \sim 2.3$, $T_1 \sim 10$. The critical Lorentz factor is $\eta_c \sim 60A_*^{-1/4}$. Assuming $t_{m,f} \sim 0.1$ day and $F_{\nu_{R,f}}(t_{m,f}) \sim 1\text{mJy}$, we obtain $\epsilon_e \sim 4.0 \times 10^{-2}$ and $\epsilon_B \sim 5$ from eqs (5) and (6). Since the solution $\epsilon_B \propto d^{-8} \zeta^{5/3} E^3 t_{m,f}^{-1} F_{\nu_{R,f}}(t_{m,f})^{-4}$ highly depends on the parameters, more accurate estimates on d , E and $F_{\nu_{R,f}}(t_{m,f})$ are required to determine it from the light curve break. If GRB 021004 is a thick shell case ($\kappa \equiv \eta/\eta_c > 1$), the reverse shock peak time is comparable to the burst duration $t_x \sim 100$ sec. From (20),

¹After the completion of our paper, we noticed that Li and Chevalier (2003) gave a detailed studied on this possibility in a recent paper.

the peak flux is $F_{\nu_R,r}(t_x) \sim 60\kappa^{-1/2}\text{mJy}$ for $\lambda \equiv \nu_R/\nu_{m,r}(t_x) > 1$, and $\sim 180\kappa^{-1}\text{mJy}$ for $\lambda < 1$. In the thin shell case ($\kappa < 1$), the peak time is $t_x \sim 100\kappa^{-4}$ sec, the peak flux is $F_{\nu_R,r}(t_x) \sim 60\kappa^5\text{mJy}$ for $\lambda > 1$, and $\sim 180\kappa^2\text{mJy}$ for $\lambda < 1$.

6. Conclusions

We have studied the optical emissions from reverse shocks for the thin and thick shell cases. The differences between this model and the ISM model are highlighted in Figure 1. In the ISM model, the prompt optical emission increases proportional to t^5 for the the thin shell case or $t^{1/2}$ for the thick shell case (Kobayashi 2000). However, in the wind model, it behaves as $t^{1/2}$ for the both cases. If a rapid brightening with an index larger than $1/2$ is caught, it could be an indication of the ISM-type GRB. The decay index of the emission is determined by the angular time delay effect in the wind model so that $\sim t^{-3}$, while it depends on the hydrodynamic evolution of the fireball ejecta in the ISM model hence $\sim t^{-2}$.

When we detect the peak time of the reverse shock emission, we can estimate the Lorentz factor at that time from eq.(13). In the ISM model, the peak time was given by a similar relation $t_x \sim (\gamma_x/\eta'_c)^{-8/3}T$ (Sari & Piran 1999a) where η'_c is a critical Lorentz factor and given by eq. (7) in Kobayashi & Zhang (2003). Additionally, if we detect the break, caused by the passage of $\nu_{m,f}$, in the late time (~ 1 hr after the burst) optical light curve, from eq. (20) we can give another constraint on the initial Lorentz factor η (see also Zhang et al. 2003 for the ISM case).

This work is supported by NASA NAG5-9192 and the Pennsylvania State University Center for Gravitational Wave Physics, which is funded by NSF under cooperative agreement PHY 01-14375.

References

- Akerlof,C.W. et al. 1999, *Nature*, 398, 400.
- Blandford,R.D. & McKee,C.F. 1976, *Phys of Fluids*, 19, 1130.
- Chevalier,R.A. & Li,Z.Y. 1999 *ApJ*, 520, L29.
- Chevalier,R.A. & Li,Z.Y. 2000 *ApJ*, 536, 195.
- Dai,Z.G. & Lu,T. 1998, *MNRAS*, 298, 87.
- Fenimore,E.E., Madras,C.D. & Nayakshin,S. 1996 *ApJ*, 473, 998.
- Fox,D.W. et al. 2003, *Nature*, 422, 284.
- Gou,L.J.,Dai,Z.G.,Huang,Y.F. & Lu,T. 2001 *A&A*, 368, 464.
- Granot,J., Piran,T. & Sari, R. 1999 *ApJ*, 513, 679.
- Heyl,J. & Perna,R. 2003, *ApJ* in press.

- Lazzati,D. et al. 2002, A&A, 396, L5.
- Li,Z.Y. & Chevalier,R.A. 2003 submitted ApJL (astro-ph/0303650).
- Ioka,K. & Nakamura,T. 2001 ApJ, 554, L163.
- Kobayashi,S 2000, ApJ, 545, 807.
- Kobayashi,S, Piran,T. & Sari,R. 1997, ApJ, 490, 92.
- Kobayashi,S, Piran,T. & Sari,R. 1999, ApJ, 513, 669.
- Kobayashi,S & Sari,R. 2000, ApJ, 542, 819.
- Kobayashi,S & Zhang,B. 2003, ApJ, 582, L75.
- Kulkarni, S.R. et al. 1999, Nature, 398, 389.
- Kumar,P. & Panaiteescu,A. 2000a, ApJ, 541, L9.
- Kumar,P. & Panaiteescu,A. 2000b, ApJ, 541, L51.
- Mészáros,P. 2001, Science, 291, 79.
- Mészáros,P. & Rees,M.J. 1997, ApJ, 476, 231.
- Mészáros,P., Rees,M.J. & Wijers,R.A.M.J. 1998, ApJ, 499, 301.
- Nakar,E.,Piran,T. & Granot,J. 2003, New Astron in press.
- Nakar,E. & Piran,T. 2003, astro-ph/0303156.
- Rhoads,J.E. 1999 ApJ, 525, 737.
- Ryde,F. & Petrosian,V. 2002 ApJ, 578, 290.
- Sari,R. & Piran,T. 1995 ApJ, 455, L143.
- Sari,R. & Piran,T. 1999a ApJ, 520, 641.
- Sari,R. & Piran,T. 1999b ApJ, 517, L109.
- Sari,R., Piran,T. & Halpern,J.P. 1999 ApJ, 519, L17.
- Sari,R., Piran,T. & Narayan,R. 1998 ApJ, 497, L17.
- Zhang,B., Kobayashi,S. & Mészáros,P. 2003, ApJ, submitted (astro-ph/0302525).

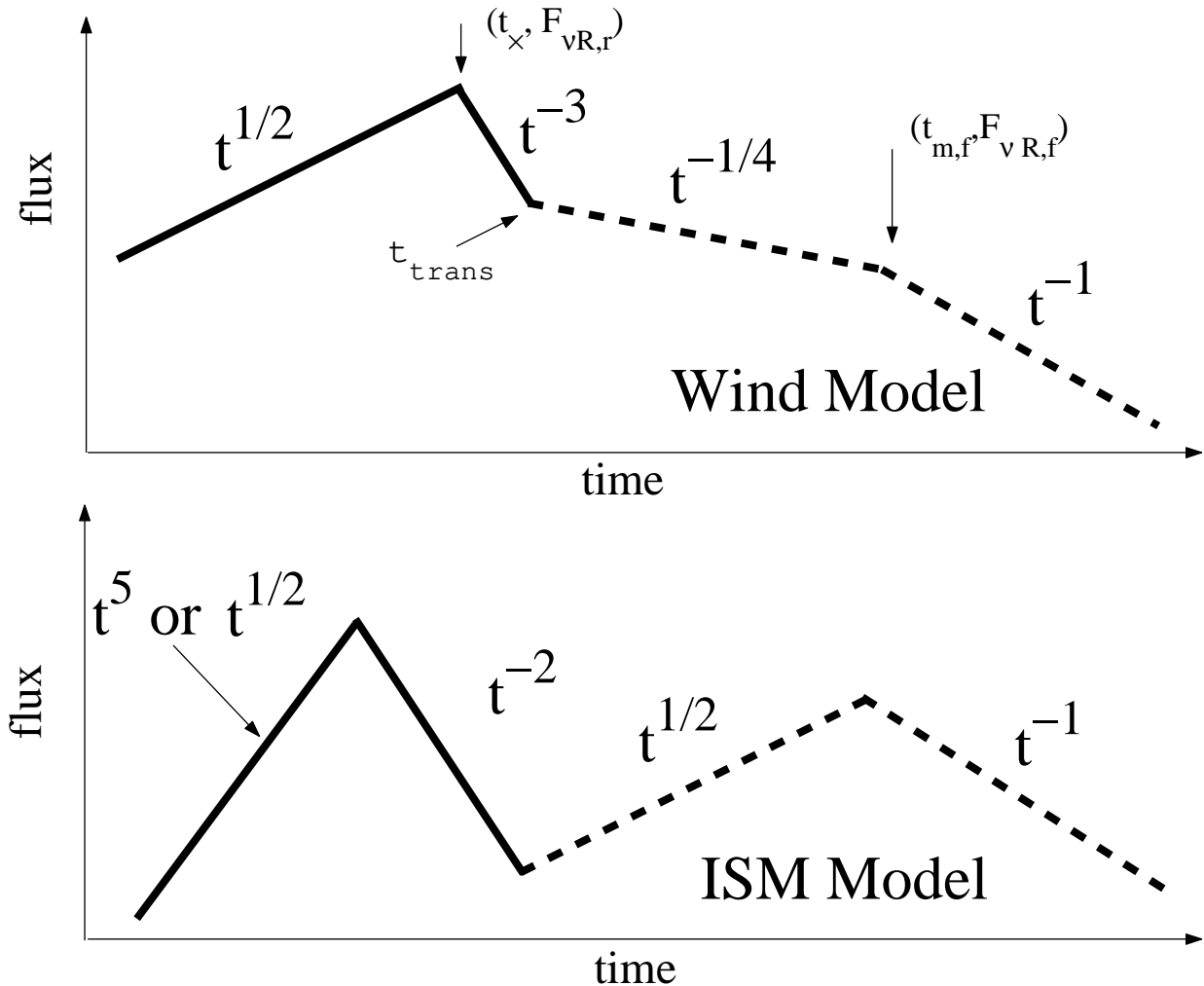


Fig. 1.— Optical light curve: Wind Model and ISM Model. Reverse Shock Emission (solid) and Forward Shock Emission (dashed).